Imaging of articular cartilage

Bhawan K Paunipagar, DD Rasalkar[1]

Department of Imaging Sciences, Global Hospitals, Mumbai, [1]Department of Radiology, Kokilaben Dhirubhai Ambani Hospital, Mumbai, India

Correspondence: Dr. Bhawan K Paunipagar, Department of Imaging Sciences, Global Hospitals, Mumbai, India.
E-mail: drbhawan@yahoo.com

Abstract

We tried to review the role of magnetic resonance imaging (MRI) in understanding microscopic and morphologic structure of the articular cartilage. The optimal protocols and available spin-echo sequences in present day practice are reviewed in context of common pathologies of articular cartilage. The future trends of articular cartilage imaging have been discussed with their appropriateness. In diarthrodial joints of the body, articular cartilage is functionally very important. It is frequently exposed to trauma, degeneration, and repetitive wear and tear. MRI has played a vital role in evaluation of articular cartilage. With the availability of advanced repair surgeries for cartilage lesions, there has been an increased demand for improved cartilage imaging techniques. Recent advances in imaging strategies for native and postoperative articular cartilage open up an entirely new approach in management of cartilage-related pathologies.

Key words: Cartilage; chondromalacia; magnetic resonance imaging

Introduction

With an increase in availability of treatment options for the articular cartilage lesions, imaging takes the front seat in determining those lesions. There has been a constant advancement in field of articular cartilage imaging.

Morphology

The articular surfaces of joints in human body are lined by hyaline cartilage. The entire role of articular cartilage is to distribute force, reduce friction, and prevent wear. It is a connective tissue of very specialized nature and configuration.[1]

Molecular Basis

Hyaline cartilage is composed of water, which constitutes about 80%, and remainder is cellular substance, intercellular matrix, and ground substance, which are essentially responsible to give firmness to cartilage. The absence of lymphatics, nerve endings and blood vessels does not allow its regeneration. When a joint is compressed, water is redistributed through cartilage cushion to absorb the compressive force whilst the overall cartilage volume may remain unchanged.[2]

There are multiple layers in articular cartilage. The superficial layer has lower proteoglycan concentration and has no permeability for water. The superficial zone may act as a cushion distributing the impact of compressive forces. If the forces remain for a prolonged period, then there is a propensity of the impact to be distributed to the deeper zones.[2]

The radial zone is the largest of all and is the deepest in location. The collagen fibers are perpendicular in orientation in upper two-thirds, whereas they are curved obliquely in the lower third. The "tidemark" junction is a thin calcified layer deep to the radial zone. In this layer, the collagen fibers anchor the underlying subchondral bone.[3]

MRI Appearance of Normal Articular Cartilage

It is an immense challenge to image the thin articular cartilage, which has the maximum thickness not beyond 4 mm with smooth curved contours. Magnetic resonance

imaging (MRI) has the privilege of being the radiological investigation with maximum promise in the evaluation of articular cartilage. The merits of MRI are its high spatial resolution and a superb soft tissue contrast, together with multiplanar facility. The sensitivity of MRI is reduced due to the partial volume averaging effects, which may often mask early chondral lesions like fissures and cartilage flaps. To ascertain the efficacy of MRI to produce high-quality images, it is very essential to optimize the spatial resolution for an appropriate signal-to-noise ratio (SNR). The availability of high field strength magnets together with dedicated surface coils and dedicated pulse sequences has taken articular cartilage imaging to a higher level.

The difference in water content between the superficial and deep layers has been thought to be responsible for the homogenous appearance of articular cartilage on MRI [Figure 1A and B].

Conventional Pulse Sequences

Common MRI sequences for cartilage constitute T1-weighted, proton density, and T2-weighted imaging sequences, with or without fat saturation, but the preferable information is expected to be better assessed on high-resolution imaging which is considered important for morphological and physiologic information. In present day practice, combination of morphologic imaging sequence with high-resolution [Figure 2] facility compatible to evaluate the matrix is preferred and is readily available.

2D Fast Spin Echo

To assess the cartilage integrity, it is preferred to have proton density and T2-weighted sequences, with and without fat saturation.[4,5] Both intermediate and T2-weighted fast spin-echo (SE) imaging sequences, with and without fat suppression have been advocated in the assessment of articular cartilage integrity[6] [Figure 3].

The disruption of ultrastructure of collagen matrix together with intra-cartilaginous water imbibement is reflected as areas of increased signal, with morphologic contour defects[7] most likely reflective of increased intra-cartilaginous free water and collagenous ultrastructure disruption.

There is a limited role of T1-weighted imaging in cartilage evaluation due to lack of good tissue contrast from the adjacent joint fluid and the articular cartilage surface, making it suboptimal for particular usage [Figure 4]. Additional shortcomings are its limitations in assessing the adjacent soft tissue structures.[8]

Proton density-weighted sequence has the feature of T1 and efficacy of T2, based upon the local concentration of the hydrogen nuclei [Figure 5]. The intact articular cartilage has low signal intensity as compared to the bright fluid signal intensity, increasing the conspicuity of the focal surface lesions[7,9] [Figure 6].

The T2-weighted imaging sequences show excellent contrast difference due to fluid-cartilage interphase, but at the expense of slightly reduced signal from the articular cartilage. T1-weighted conventional SE sequences have high SNR and good spatial resolution, but poor contrast between cartilage and joint fluid.[10]

Fat Suppression Techniques

To improve the dynamic range of signal intensity from an image, fat suppression sequence is implemented in the routine protocol for cartilage imaging pulse sequences. There is better detection of minor signal intensity modifications.[11,12] A T1-weighted inversion recovery sequence, termed as short tau inversion recovery (STIR), is another technique by which the effect of fat suppression is obtained. Combination of fat suppression together with three-dimensional (3D) spoiled gradient echo sequence only depicts the articular cartilage as a bright structure.
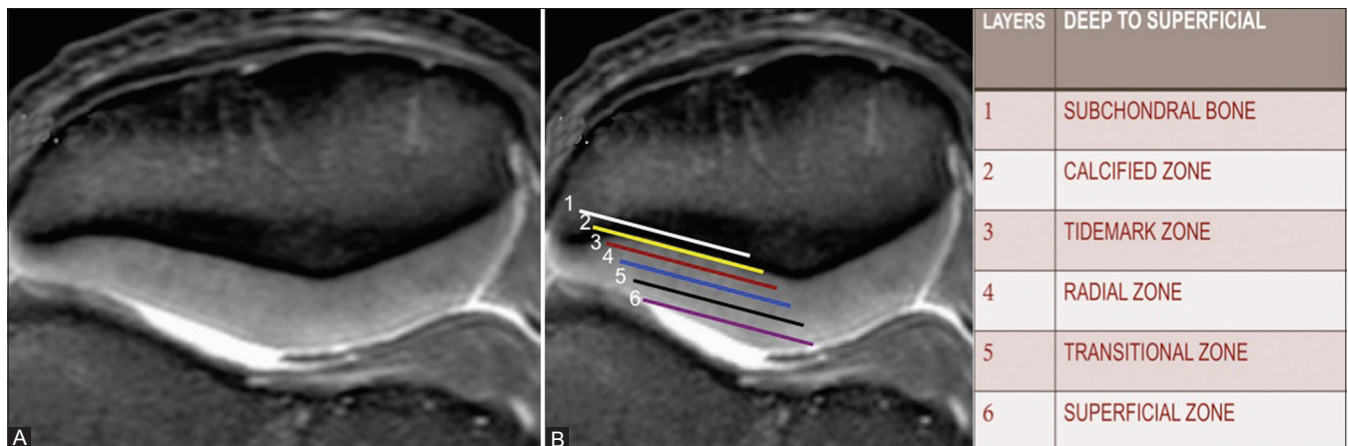

LAYERS	DEEP TO SUPERFICIAL
1	SUBCHONDRAL BONE
2	CALCIFIED ZONE
3	TIDEMARK ZONE
4	RADIAL ZONE
5	TRANSITIONAL ZONE
6	SUPERFICIAL ZONE

Figure 1 (A and B): (A) Coronal PD FS MR image in 32 year old man with arthroscopically normal retropatellar articular cartilage. (B) A graphic depiction of layers of articular cartilage on a MRI image as identified on histology

The sequence with the best possible potential to assess the articular cartilage accurately is spoiled gradient echo sequence (SPGR).[13]

Volumetric Sequences

Optimal spatial resolution of images can be obtained by acquiring thinner slices (0.2 to 0.4 mm thickness) producing isotropic voxels with equal dimensions in the three planes. The advantage of volumetric image acquisition is that it facilitates multiplanar reformation without loss of the spatial resolution,
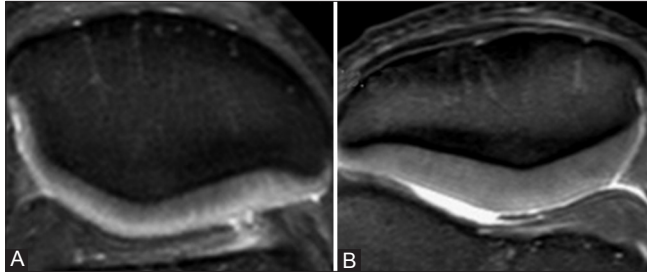

Figure 2 (A and B): Axial FS T2W images of the patella targetted for cartilage imaging (A) large FOV (B) Small FOV. Note better delineation of chondral morphology in retropatellar cartilage when images obtained at a smaller FOV. Similarly, use of a small FOV for superficial structures like joints may help us improve spatial resolution and conspicuity of chondral based lesions
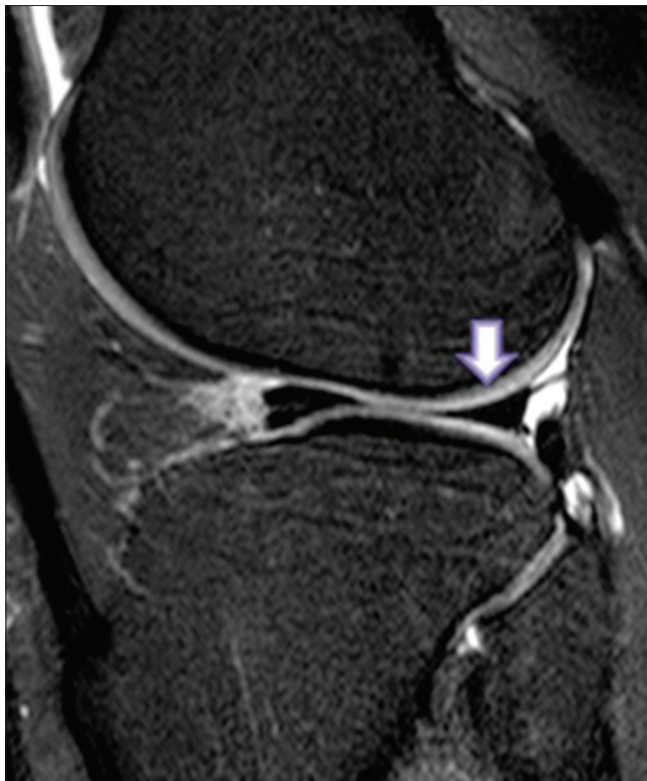
allowing a better quantitative measurement of cartilage abnormalities and reducing partial volume artifacts.[14]

Gradient Echo Sequences

Gradient echo sequences allow volumetric image acquisition with reduced imaging times and improved spatial resolution. Technically, a refocusing pulse separates two or more gradient echoes, eventually combining the echoes to generate an image.[15,16] Gradient-recalled echo (GRE) sequences suffer from a potential fallacy, as they are unusually sensitive and susceptible to intravoxel dephasing, especially in patients with previous surgical intervention or some hardware placement[13] [Figure 7].

3D Fast Spin Echo Imaging

The structures that are oblique in course or some small structures that extend into multiple slices pose a great amount of problem. To tackle this problem, there is an advent of 3D sequences which are fast SE images equipped with flip angle modulation reducing blurring and imaging times, making isotropic imaging possible. Such 3D images have an isotropic resolution and an advantage of multiplanar reformats.[17,18]
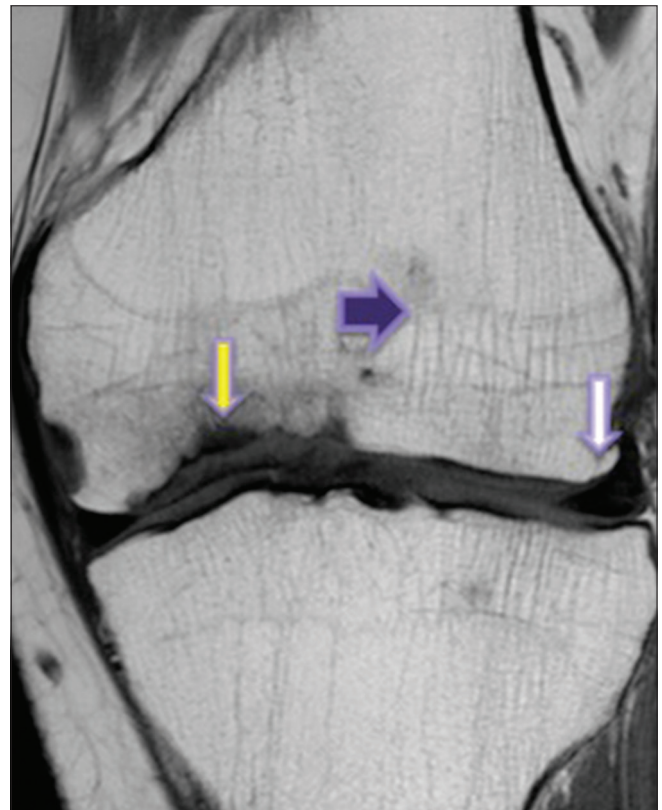

Figure 3: Sagittal FS T2W FSE image of knee joint. The articular cartilage appears hyperintense. Note excellent morphological detail of articular cartilage. The other structures of knee joint can also be identified. However finer morphology of articular cartilage along tidemark junction (arrow) is compromised

Figure 4: Coronal T1W image of knee joint. The articular cartilage appears hypointense. The bone details like bone trabecular pattern (blue arrow), marginal osteophytosis (white arrow) and subchondral sclerosis (yellow arrow) are nicely depicted. However, there is compromised information of articular cartilage
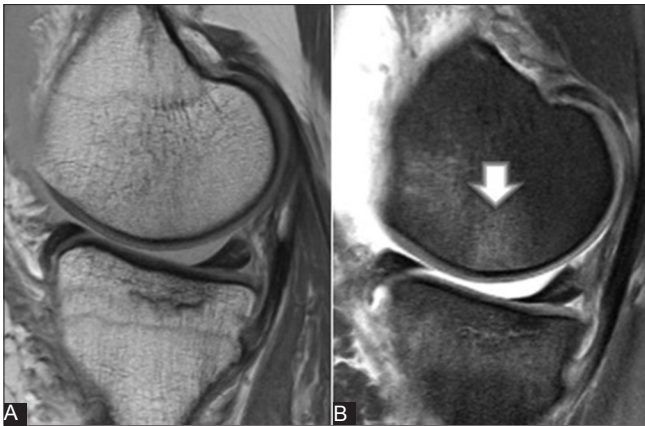
Figure 5 (A and B): Sagittal PD-weighted non-FS (A) and FS (B) images of knee reveal efficacy of 2D FSE sequence to depict articular cartilage. The non-FS image actually has a better delineation of articular cartilage and subchondral bone, except of subtle marrow edema (arrow), which is better appreciated on FS images, but suffers with mild image blur

SPGR

Spoiled gradient echo sequences such as SPGR or fast low angle shot (FLASH) provide T1-weighted images with better contrast between cartilage (hyperintense) and intra-articular fluid (hypointense).[19,20] Standard SE MRI has a lower accuracy as compared to the fat-suppressed SPGR. The sensitivity of the sequence approaches 93%, with articular cartilage appearing bright and remainder of the structures appearing relatively dark[21,22] [Figure 8]. 3D SPGR is recommended by the International Cartilage Repair Society (ICRS) as a standard sequence in imaging for evaluation of the articular cartilage lesions, especially in post cartilage repair status. The images are primarily T1-weighted sequences obtained at a low flip angle. The disadvantages are longer acquisition times and inadequacy to depict surface defects as well as the other joint structures. Finally, 3D gradient echo methods are less useful for the diagnosis of ligament or meniscal tears than SE techniques. Despite these limitations, 3D SPGR imaging is considered the standard for morphologic imaging of cartilage[23] [Figure 9].

MR Arthrography

Post cartilage repair, MR arthrography (MRA) is recommended in evaluation of cartilage integrity. The instilled contrast outlines cartilage defects and their contours. A small amount of 2mmol/l gadolinium contrast (Dotarem, Guerbet LLC, USA) mixed with saline is injected within the joint space to increase its sensitivity to detect cartilage abnormalities.[24,25] MRA has been shown to be more sensitive than the standard 3D T2-weighted gradient echo sequences for the detection of cartilage lesions[26] [Figure 10].

Pathomechanics

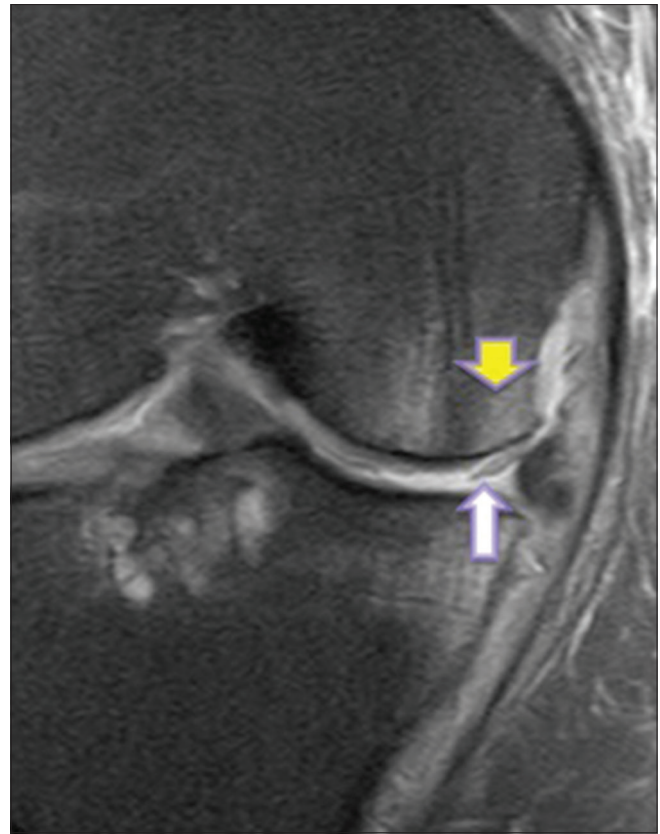Chondral lesions in their early stages result in contour

Figure 6: Hyperextension injury of knee sustained in a 20 year old man. Coronal FS PD-weighted image of knee joint shows a mildly displaced chondral flap (white arrow) involving the weight-bearing surface of the medial femoral condyle. There are kissing bone marrow contusions of the medial aspect of the anterior tibia and femur (yellow arrow) secondary to the hyperextension injury. Valgus stress occurring at the hyperextension injury resulted in the medial location of the kissing contusions

changes in the form of swelling, fibrillation, and surface irregularity, together with cartilage thinning.

Development of various MRI imaging techniques allows morphologic assessment of cartilage, quantification of its volume, and evaluation of its biochemical composition. It is considered that thinning of articular cartilage is a normal age-related phenomenon and cartilage thickness is inversely proportional to the age of the patient.[27]

Degenerative Disease

Chronic stress-related microtrauma to articular cartilage and bone results in arthrosis and osteoarthritis, which involve diffuse chondropathy, osteophytes, eburnation of the bone surface, and subchondral changes[28] [Figure 11].

Trauma

Microtrauma-related articular fractures and thinning of articular cartilage is the common etiopathogenesis of osteoarthrosis. Chondral fractures are well demonstrated at arthroscopy in patients with hemarthrosis.[28]
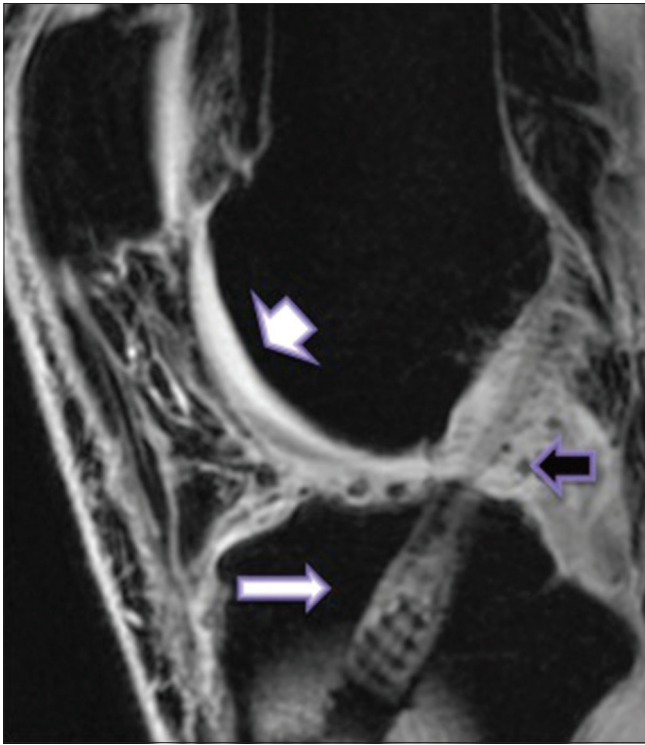
Figure 7: A 3D GRE, sagittal plane image of knee joint revealing articular cartilage. Note excellent details of articular cartilage. (short arrow) The additional advantage of this sequence is in imaging of joints with prior interventions or any grafts or screws fixations. (long arrow) Note the tiny blooming intensities (black arrow) around the BPB graft, likely postoperative bone fragments
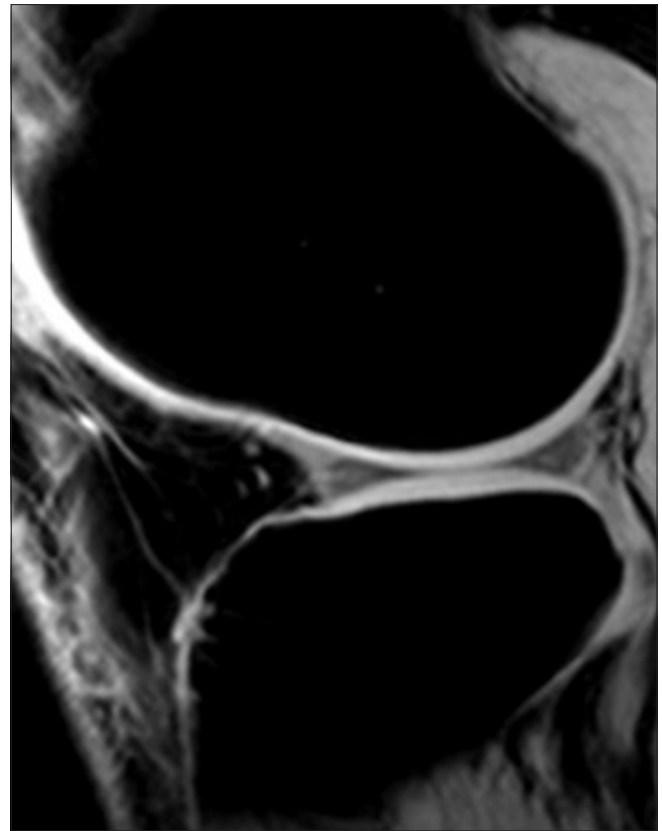

Figure 8: Sagittal 3D SPGR (TR/TE 14.1/5 ms) at flip angle 60° of knee provides excellent contrast between cartilage and subchondral bone along signal-intensity cartilaginous surfaces in tibiofemoral compartments

On MRI, chondral pathologies are depicted as areas of focal chondral defects or deeper fractures involving the subchondral bone [Table 1].

Chondral lesions are graded based upon the thickness of articular cartilage disruption. The cartilage may undergo swelling (focal or diffuse) represented as an area of hyperintensity on fluid-sensitive sequence [Figure 12]. Focal disruption of cartilage may be a linear cleft or multiple linear clefts representing fissures of variable depths [Figure 13]. Full-thickness cartilage separation from the tidemark zone results in chondral flap injuries or delamination of articular cartilage [Figure 14]. Associated with injury to articular cartilage, there may often be injury to subchondral bone, which may be represented as bone marrow edema, subchondral bone fracture, or displaced fracture [Figure 15].

Osteochondral lesions need a further detailed description based upon location, size, and depth of lesion [Figure 16A and B].

New Pulse Sequences

To date, no one acquisition sequence has been proven to be ideal, although the majority of publications on volume

Table 1: Modified outerbridge classification

Grade	MRI features	Arthroscopy	Histopathology
I	FS PD focal areas of hyperintensity within normal contour	Softening by arthroscopy	Focal basal degeneration
II	FS PD fissure or blister-like swelling of articular cartilage extending to surface	Fissuring and fibrillation within soft areas of articular cartilage (1-2 mm deep)	-
III	FS PD focal ulcerations and "crab meat" lesions	Partial thickness cartilage loss >2 mm deep	-
IV	FS PD full-thickness cartilage loss with underlying bone reactive changes	Ulceration with exposed subchondral bone	

FS PD: Fat saturated Proton density

and thickness measurements have used the 3D T1-weighted SPGR sequence.[29,30]

These methods include the following:
- Steady-state free precession (SSFP) [fast imaging employing steady-state acquisition (FIESTA)]
- True fast imaging with SSFP (true-FISP)
- Balanced fast field echo and its variant, fluctuating equilibrium MRI (FEMR)

- Multi-echo techniques such as dual excitation in the steady state [dual-echo steady state (DESS)]; driven equilibrium techniques such as driven equilibrium Fourier transform (DEFT) and fast recovery fast spin echo; echo-planar techniques such as 3D echo-planar imaging with fat suppression and 3D DEFT; and 3D fast SE methods.[31]

Diffusion MRI Techniques

The movement of water within extracellular matrix (ECM) of articular cartilage has been considered a potentially useful measure to assess biochemical constitution of the articular cartilage.

DWI

There is alteration of the magnetic field gradients due to the movement of the water. Eventually, this water movement has been calculated as a b-factor, which has an echo time characterizing the degree of T2 weighting and is mapped pixel by pixel.[32,33] Diffusion-weighted imaging (DWI) has been demonstrated as a potential method for assessing cartilage degeneration *in vivo*[34] and monitoring its repair following surgery.[35]
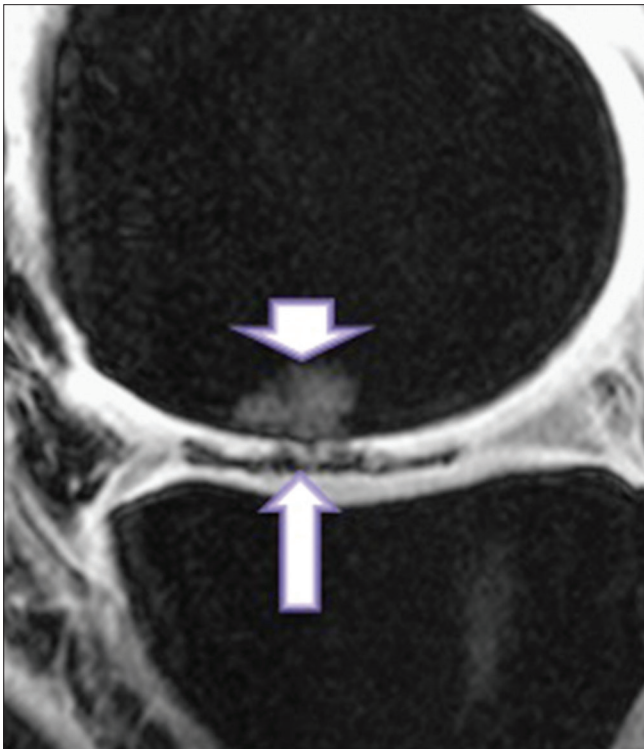
Figure 9: A 46 year old male volunteer with knee pain. Sagittal images of knee joint show superficial cartilage fissure (long arrow) within medial femoral condyle. Note that superficial cartilage lesion is more conspicuous on SPGR image. This is classically termed as 'crab meat' appearance. Additionally, small amount of marrow edema (short arrow) is also appreciable. According to Modified Outerbridge classification, crab meat appearance is categorized as grade 3 chondral lesions

ADC

Apparent diffusion coefficient (ADC) determines the interaction between water molecules in relation to the adjacent environment. This coefficient has been measured in articular cartilage, suggesting integrity of tissue morphology. An increased diffusivity suggests structural disintegration of the ECM and, hence, can be readily utilized as a potential method in post cartilage repair imaging[36,37] with increased diffusivity linked to structural degradation of the ECM.

DTI

Orientation of the collagen fibrils in the ECM of the articular cartilage has been studied using diffusion tensor imaging (DTI). The disruption of the collagen network is mapped on DTI. But its drawbacks are intricate data analysis and a longer duration of image acquisition.[38] DTI has been used to study the effects of compression on the cartilage collagen network.[39]

DESS

DESS imaging has proven useful for the evaluation of cartilage imaging and 3-mm slices can be acquired in about 6 min. Initial studies of cartilage morphology have been performed using DEFT imaging,[40,41] but this technique has not been conclusively proven to be superior to 2D approaches [Figure 17].

Balanced SSFP Imaging

It is an efficient 3D MR sequence obtained with a high signal and fast acquisition times, employing a precision of steady state [Figure 18]. A higher resolution is obtained by multiple acquisitions at an expense of increased scanning time.[42]

Several studies have shown the utility of the balanced SSFP (bSSFP) sequence for imaging articular cartilage.[43-45] Because of the bright synovial fluid and 3D nature of the acquisition, bSSFP may also be useful for imaging internal
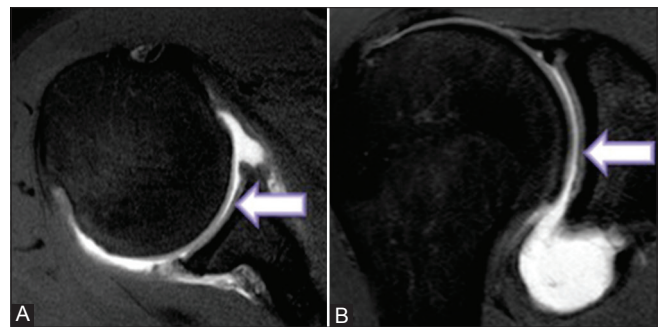
Figure 10 (A and B): A T1 W FS Axial (A) and coronal (B) image of MR Arthogram. In addition to routine information of glenoid labrum, we can assess articular cartilage well. The presence of intra-articular gadolinium contrast helps us in assessment of cartilage morphology

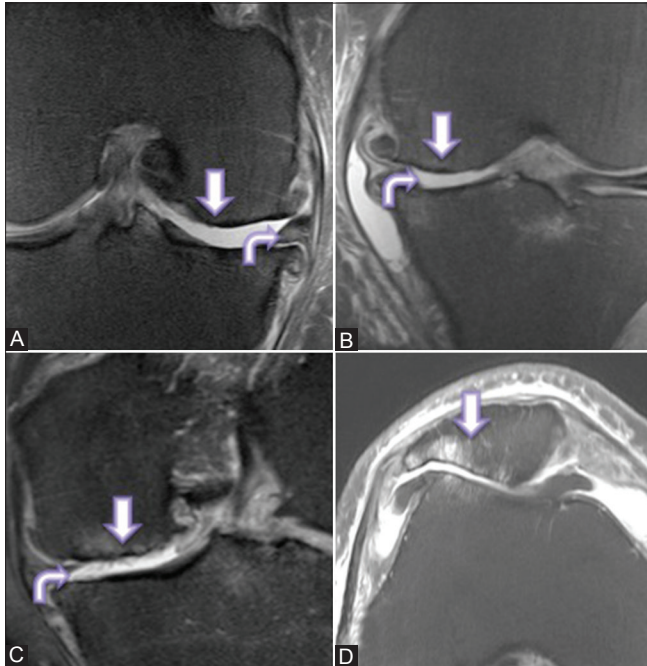derangements of other structures including ligaments and menisci.[46]

Figure 11 (A-D): Multiplanar FS PD-weighted images in a 56 year old woman who previously underwent arthroscopic partial medial meniscectomy. MRI images of knee joint show established osteoarthrosis in medial-lateral femorotibial and patellofemoral articulation. There is a near-complete loss of articular cartilage covering weight bearing surfaces of femoral and tibial condyles as well as non-weight bearing surface of patellofemoral articulation exposing subchondral bone. There are established marginal osteophytosis and subchondral bone sclerosis
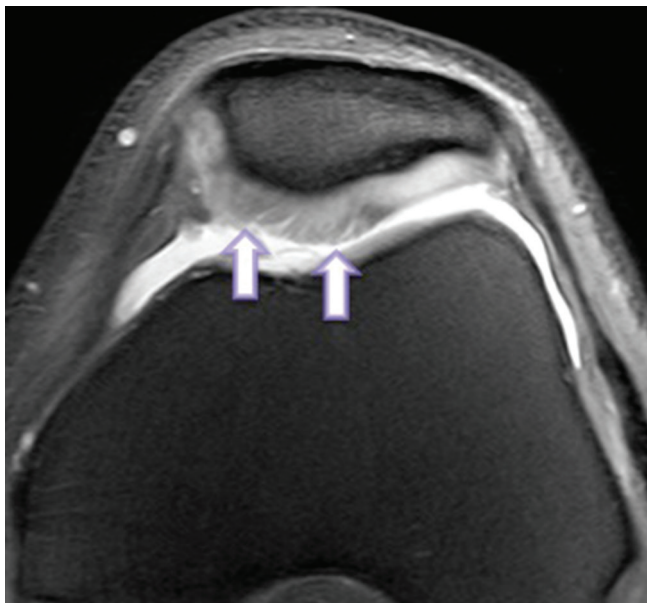

Figure 13: Axial 2D fat-saturated PD-weighted fast spin-echo image of knee joint in a 47 year old man shows arthroscopically confirmed superficial cartilage fibrillation (arrows) categorized as grade 2 cartilage lesion

Relaxation Time Mapping

Water molecules excite and relax reaching back to the equilibrium state. T1 and T2 relaxation times describe the exponential time constants obtained due to movement of the water molecules in a tissue at the field strength.

T1 Relaxation

During the spin, the rate at which the nuclei diffuse the energy to the surroundings following the excitation is determined by T1 relaxation, which is sensitive to the macromolecular structure of the cartilage matrix.[47,48]

T2 Relaxation

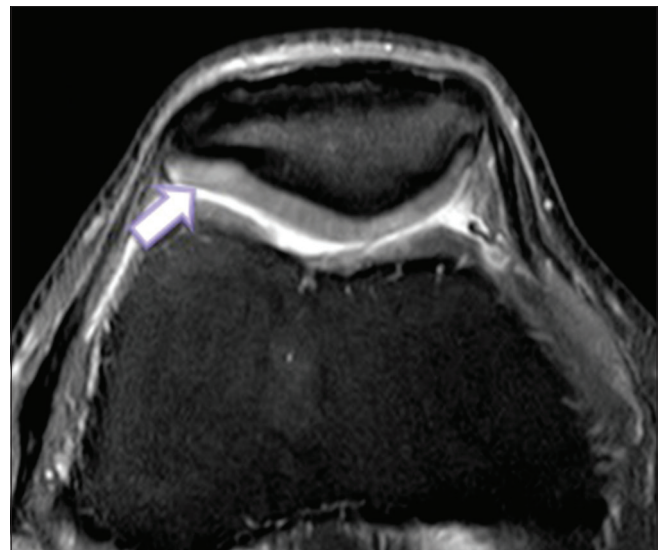The function of the water and collagen content of the

Figure 12: Axial image acquired with multiple-echo data image combination sequence shows grade 1 cartilage lesion. There is a focal area of chondral softening revealed as an area of focal hyperintensity (arrow) within the articular cartilage
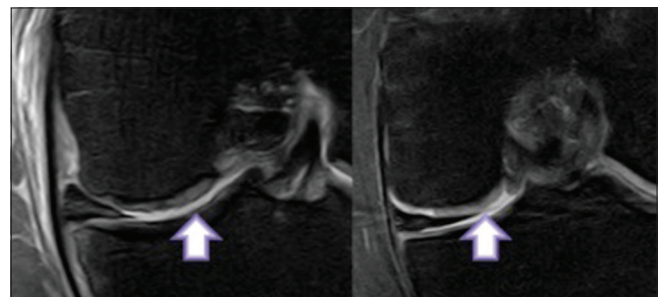

Figure 14: Coronal FS PD weighted image of the knee reveals a grade 2 chondromalacia of the weight-bearing surface of the medial femoral condyle. (arrows) Note the fibrillar contour of cartilage surface in a 36 year old man with surgically confirmed superficial partial-thickness cartilage lesion

articular cartilage matrix is determined by the T2 relaxation time. The T2 relaxation values are variable, based upon the articular cartilage thickness comparable to the distribution of the water and proteoglycans in the ECM.[49] The measured distribution of the T2 relaxation is depicted as areas of increased or decreased content of the water directly proportional to the degree of the cartilage disintegration.[50] It is of utmost importance to select the MRI technique that has high accuracy to measure T2 relaxation [Figure 19].

T1rho Imaging

T1rho imaging is a potentially sensitive MRI technique to detect early depletion of the proteoglycans in the ECM. It detects the alterations in the relaxation of the spins in a magnetic field. This technique is different from T2 mapping that determines the changes in the collagen architecture; moreover, the T1rho value variations are remarkably larger in cases of osteoarthrosis, offering a wider spectrum of disease detection.[51-54]

Physiologic MRI of Cartilage

Physiologic MRI helps to explore the internal architecture of the articular cartilage by the use of collagen and proteoglycan arrangement. There is a combination of 70% water and the remainder consisting of type 2 collagen fibers and proteoglycans. The concept of positively charged sodium ions from the collagen fibers interacting with the negatively charged gadolinium contrast particle indirectly depicts the concentration of the proteoglycans.
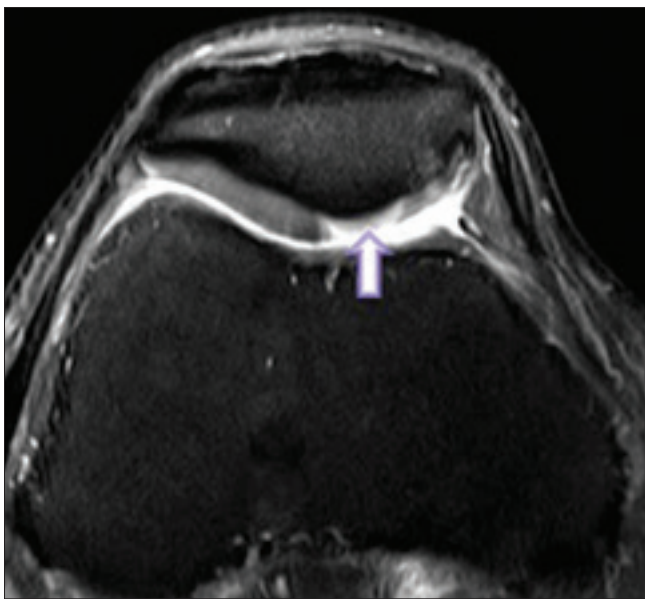

Figure 15: Axial fast spin-echo PD FS image in 39 year old man reveals a wide area of full-thickness chondromalacia (arrow) involving the median ridge and the medial patellar facet categorized as grade 3 lesion (fissuring of cartilage to level of subchondral bone) in the posterior aspect of the patella. The subchondral bone is not exposed, which discriminates this lesion from a grade 4 lesion

The interaction is determined by the magnetization transfer and can be readily identified under 1.5 and 3 T systems.[13]

Delayed Gadolinium-enhanced MRI of the Cartilage

Early degeneration of articular cartilage occurs in the form of degradation of proteoglycans in ECM.[55] There is a direct relationship of the contrast-enhanced T1 and glycosaminoglycan (GAG) concentration affected by patient's body mass index. There is an effective penetration of contrast into area of cartilage, which has a disrupted concentration of GAG. A normal articular cartilage has a low gadolinium diethylenetriaminepentaacetic acid GdDTPA concentration, whereas areas of damaged articular cartilage allow contrast material to trickle in areas of delayed hyperenhancement of articular cartilage. Imaging-wise, a double dose of the Gd contrast material is injected intravenously and images are acquired after a delay of about 2 h, allowing sufficient time for contrast to percolate into areas of damaged collagen.[56] The concentration of GAG is inversely proportional to concentration of Gd contrast on T1W imaging. A T1 map is plotted based on contrast concentration indirectly quantifying GAG in cartilage. Delayed gadolinium-enhanced MRI of cartilage (dGEMRIC) has a significant promise to assess biochemical changes in articular cartilage morphology and may reflect early cartilage degeneration or maturation based upon concentration of GAG.[56]

Sodium MRI

Articular cartilage has a high concentration of sodium. Taking advantage of this, sodium MRI has been brought in for cartilage imaging. The areas of proteoglycan depletion are represented as areas of high sodium concentration. This
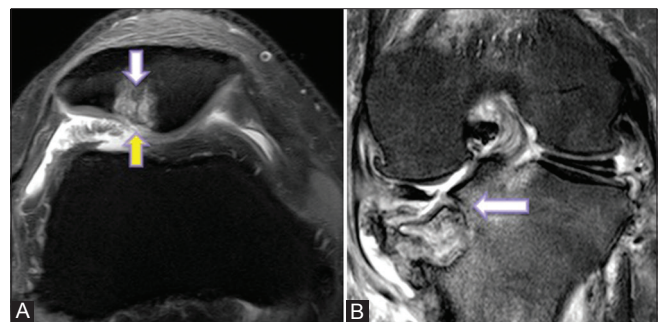

Figure 16 (A and B): (A) Axial FS PD-weighted sequence (TR/TE, 884/26; flip angle, 30°) image of knee joint shows grade 4 chondromalacia (yellow arrow) of articular cartilage in median patellar ridge and lateral patellar facet. The remainder of articular cartilage is irregularly thinned out. There is a moderate amount of edema of marrow in subchondral aspect (white arrow). (B) Coronal FS PD weighted images of an adult patient. There is a large osteochondral lesion involving weight-bearing surface of medial tibial condyle. There is a moderate depression of this osteochondral lesion (arrow) with moderate surrounding marrow edema

technique is considered an alternative method to dGEMRIC to assess focal cortical defect. Triple-quantum-filtered imaging of sodium in cartilage, which may be even more sensitive to early changes than sodium imaging, is also possible.[57]
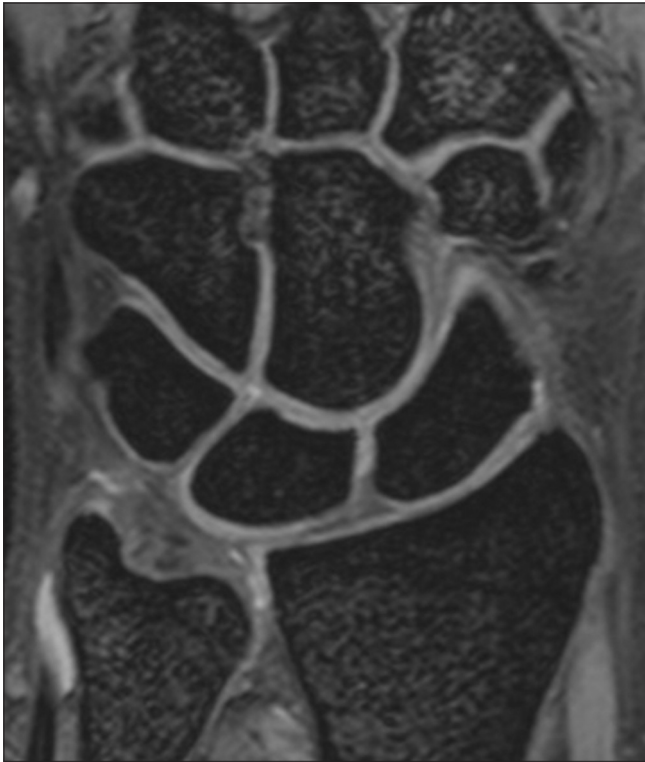

Figure 17: Sagittal water selective 3D DESS imaging of wrist (TR/TE 14.1/5 ms). At the flip angle of 60°, there is highest signal intensity of articular cartilage with highest contrast-to-noise ratio of cartilage. Note excellent details of articular cartilage. Note that the details of subchondral bone are compromised

Figure 19 (A-C): Axial T1 TSE image (600/6.6, NEX 2.0, 180° flip angle) of the retropatellar cartilage obtained in a volunteer reveals morphologically normal cartilage (A). Corresponding T2 maps for the early (B) and late unloading (C). Note no visible differences over time

3 T versus 1.5 T

SNR is directly proportional to magnetic field strength [Figure 20]. A greater spatial resolution with equal imaging time and SNR is obtained with higher magnetic strengths.[58]

Higher field strength magnets have a potential for an improved articular cartilage imaging. Lower field

Figure 18: 47 year old male volunteer with knee pain. Sagittal balanced steady-state free precession (bSSFP) image of knee joint (0.3 mm isotropic resolution and 8 minute scanning time) shows superficial partial-thickness cartilage thinning (arrow) on anterior weight bearing surface of lateral femoral condyle
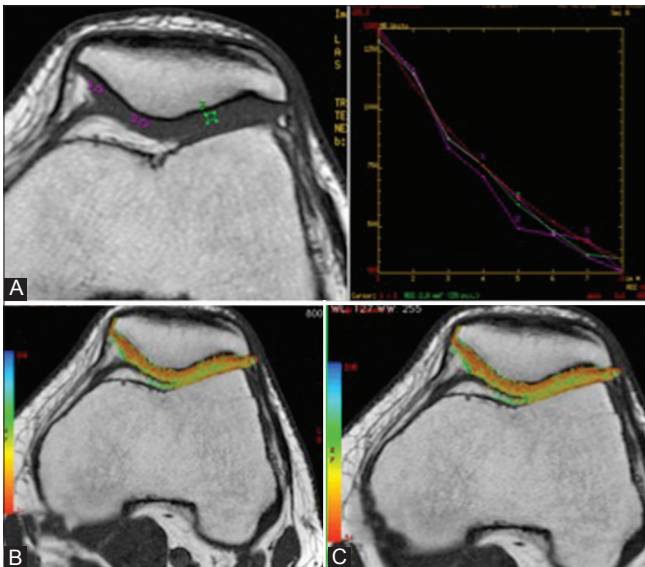

Figure 20 (A and B): Axial 2D FS PD TSE images obtained at a 3T (A) and 1.5T (B) respectively. Note the excellent contrast differentiation among cartilage surfaces, synovial fluid, and subchondral bone, as well as variation of signal intensity within the cartilage. It is very obvious that high field 3T magnet (a) depicts the finer details of the articular cartilage to a greater extent as opposed to a magnet of lesser strength. If all parameters remain similar, the voxel size in a 1.5 T remains 276% larger than in 3

strength magnets reduce the benefits, especially in non-fat-suppressed methods. With higher field magnets, there is an increase in T1 relaxation times together with increase in frequency differences amongst cartilage, water and marrow fat. There is a twofold increase in SNR at the same spatial resolution and imaging time or a reduction by fourfold in the imaging time.

Discussion

MRI non-invasively provides significant information regarding contents of articular cartilage and its macromolecular structure. Availability of cartilage-specific sequence allows sensitive prediction of the mechanical integrity of the articular cartilage.[59]

Morphologic assessment of articular cartilage by MRI specific sequences provides an excellent tissue contrast that gives detailed information of early chondral-based lesions or pathologies. An appropriate cartilage-based sequence should provide details of cartilage morphology, cartilage thickness, volume, and any disturbances of internal signal intensities. Many of the MRI parameters can assess macromolecular detail, biochemical configuration, and the physiological changes of cartilage.[60] In addition to morphologic assessment, tissue parameters that can be measured by MRI techniques also have the potential to provide biochemical and physiologic information about cartilage.

Physiological MRI imaging sequences are available for hyaline cartilage, which readily give information about composition of articular cartilage, collagen matrix, and GAGs. On the other hand, conventional MRI sequences do not help much in cartilage assessment as they typically lack required spatial resolution or information about cartilage physiology.

Hyaline cartilage is made up of chondrocytes and water,

together with macromolecules such as glycoproteins, proteoglycans, and collagen. The various layers within articular cartilage are histologically categorized as superficial, transitional, and deep zone, based upon variations in orientations of collagen fibers and number of chondrocytes.

Current musculoskeletal MRI protocols include multiple planes of 2D FSE and 3D gradient echo images. In this article, current understanding of MRI appearance of articular cartilage and its relationship to microscopic and macroscopic structure of articular cartilage, the optimal pulse sequences to be used, and appearance of both degenerative and traumatic chondral lesions are discussed. Improvements have been made in morphologic imaging of cartilage in terms of contrast, resolution, and acquisition time. These improvements allow detailed maps of cartilage surface to be developed that can be used to quantify both thickness and volume. The choice of a particular protocol for imaging articular cartilage depends greatly on patient factors. Currently available MRI imaging techniques for evaluating morphologic and compositional characteristics of articular cartilage in knee in clinical and research settings are also reviewed in the article.

Disorders may involve either the cartilage (chondral disorder), subchondral bone (subchondral bony disorder), or both (osteochondral disorder). Injury of bone is often associated with cartilage damage and vice versa.

Recent MRI techniques include GRE sequences, cartilage mapping, and dGEMRIC sequences. Use of contrast medium either injected intravenously or within the joint is showing promise in evaluation of cartilage damage and GAG glycoprotein content.[60]

MRI is the imaging method of choice in evaluation of cartilage lesions and alterations in their morphologic composition.

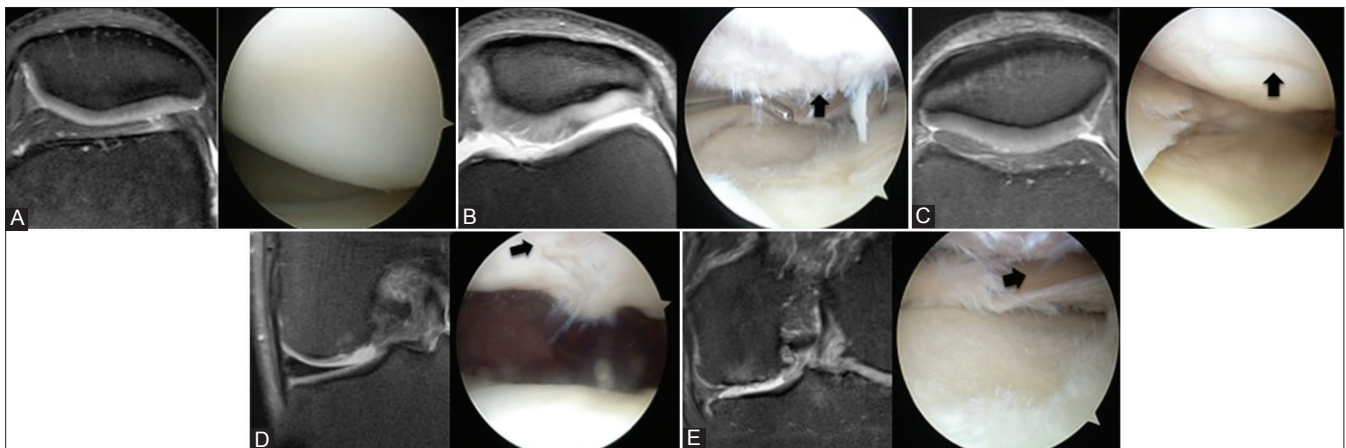**Figure 21 (A-E):** MRI images depicting grading of articular cartilage lesions based upon Modified Outerbridge classification. Grade 0 (21A, normal articular cartilage), grade 1 (21B, chondral surface fibrilation), grade 2 (21C, partial thickness chondral lesion), grade 3 (21D, full thickness cartilage lesion reaching the bone), grade 4 (21E, full thickness cartilage lesion exposing the subchondral bone)

It is a very useful investigation in cartilage-based pathologies as well as in follow-up to assess treatment response. Compositional assessment techniques include T2 mapping, delayed gadolinium-enhanced MR imaging of cartilage (dGEMRIC), T1 imaging, sodium imaging, and DWI.

There are various modifications in MRI protocols and parameters which have been formulated to alter the SNR amongst structures surrounding articular cartilage in relation to cartilage proper, indirectly allowing us to ascertain subtle cartilage-based lesions [Figure 21]. MRA of knee helps to increase sensitivity for cartilage lesions and for detection of intra-articular bodies and their donor sites, but it is also not routinely performed. Indications for MRA include evaluation of articular cartilage.

Conclusion

There are several variations in the existing imaging techniques with alterations in the imaging parameters. Numerous variations of these imaging techniques exist, with the imaging parameters and acquisition sequences varying between centers on the basis of multiple factors, including user preferences and the potential strengths and weaknesses of the available vendor hardware platforms. In general, practical MRI protocols for the evaluation of hyaline articular cartilage include at least one cartilage-sensitive sequence obtained in the sagittal plane. Supplemental acquisitions or reformatting of 3D data sets in the axial and coronal planes may help to optimize evaluation of patellar cartilage and central weight-bearing aspects of the femoral condyles and tibial plateau, respectively.

References

1. Buckwalter JA, Mankin HJ. Articular cartilage: Tissue design and chondrocyte-matrix interactions. Instr Course Lect 1998;47:477-86.
2. Lehner KB, Rechl HP, Gmeinwieser JK, Heuck AF, Lukas HP, Kohl HP. Structure, function, and degeneration of bovine hyaline cartilage: Assessment with MR imaging in vitro. Radiology 1989;170:495-9.
3. Rubenstein JD, Kim JK, Morova-Protzner I, Stanchev PL, Henkelman RM. Effects of collagen orientation on MR imaging characteristics of bovine articular cartilage. Radiology 1993;188:219-26.
4. Akeson WH, Amiel D, Gershuni DH. Articular cartilage physiology and metabolism. In: Resnick D, editor. Diagnosis of bone and joint disorders. 3rd ed. Philadelphia, PA: Saunders; 1995. p. 769-90.
5. Gray ML, Burstein D, Lesperance LM, Gehrke L. Magnetization transfer in cartilage and its constit- uent macromolecules. Magn Reson Med 1995;34:319-25.
6. Mosher TJ, Dardzinski BJ, Smith MB. Human articular cartilage: Influence of aging and early symptomatic degeneration on the spatial variation of T2-preliminary findings at 3T. Radiology 2000;214:259-66.
7. Bredella MA, Tirman PF, Peterfy CG, Zarlingo M, Feller JF, Bost FW, et al. Accuracy of T2-weighted fast spin-echo MR imaging with fat saturation in detecting cartilage defects in the knee: Comparison with arthroscopy in 130 patients. AJR Am J Roentgenol 1999;172:1073-80.
8. Vallotton JA, Meuli RA, Leyvraz PF, Landry M. Comparison between magnetic resonance imaging and arthroscopy in the diagnosis of patellar cartilage lesions: A prospective study. Knee Surg Sports Traumatol Arthrosc 1995;3:157-62.
9. Potter HG, Linklater JM, Allen AA, Hannafin JA, Haas SB. Magnetic resonance imaging of articular cartilage in the knee. An evaluation with use of fast-spin-echo imaging. J Bone Joint Surg Am 1998;80:1276-84.
10. Loeuille D, Olivier P, Mainard D, Gillet P, Netter P, Blum A. Review: Magnetic resonance imaging of normal and osteoarthritic cartilage. Arthritis Rheum 1998;41:963-75.
11. Totterman S, Weiss SL, Szumowski J, Katzberg RW, Hornak JP, Proskin HM, et al. MR fat suppression technique in the evaluation of normal structures of the knee. J Comput Assist Tomogr 1989;13:473-9.
12. Chandnani VP, Ho C, Chu P, Trudell D, Resnick D. Knee hyaline articular cartilage evaluated with MR imaging: A cadaveric study involving multiple imaging sequences and intraarticular injection of gadolinium and saline solution. Radiology 1991;178:557-61.
13. Gold GE, Chen CA, Koo S, Hargreaves BA, Bangerter NK. Recent advances in the articular cartilage. AJR Am J Roentgenol 2009;193:628-38.
14. Lang P, Zhao L, Zou K, Winalski C, Warfield S, Jolesz FA. Cartilage imaging at 3.0T: Comparison of standard 3D SPGR with 3D spectral spatial SPGR and 3D FSE sequences. Presented at 89th Scientific Assembly and Annual Meeting of the Radiological Society of North America, Chicago, IL; 2003.
15. Recht MP, Piraino DW, Paletta GA, Schils JP, Belhobek GH. Accuracy of fat-suppressed three-dimensional spoiled gradient-echo FLASH MR imaging in the detection of patellofemoral articular cartilage abnormalities. Radiology 1996;198:209-12.
16. Cicuttini F, Forbes A, Asbeutah A, Morris K, Stuckey S. Comparison and reproducibility of fast and conventional spoiled gradient-echo magnetic resonance sequences in the determination of knee cartilage volume. J Orthop Res 2000;18:580-4.
17. Busse RF, Brau AC, Vu A, Michelich CR, Bayram E, Kijowski R, et al. Effects of refocusing flip angle modulation and view ordering in 3D fast spin echo. Magn Reson Med 2008;60:640-9.
18. Busse RF, Hariharan H, Vu A, Brittain JH. Fast spin echo sequences with very long echo trains: Design of variable refocusing flip angle schedules and generation of clinical T2 contrast. Magn Reson Med 2006;55:1030-7.
19. Disler DG, McCauley TR, Kelman CG, Fuchs MD, Ratner LM, Wirth CR, et al. Fat-suppressed three-dimensional spoiled gradient-echo MR imaging of hyaline cartilage defects in the knee: Comparison with standard MR imaging and arthroscopy. AJR Am J Roentgenol 1996;167:127-32.
20. Disler DG, McCauley TR, Wirth CR, Fuchs MD. Detection of knee hyaline cartilage defects using fat-suppressed three-dimensional spoiled gradient- echo MR imaging: Comparison with standard MR imaging and correlation with arthroscopy. AJR Am J Roentgenol 1995;165:377-82.
21. Recht MP, Piraino DW, Paletta GA, Schils JP, Belhobek GH. Accuracy of fat-suppressed three-dimensional spoiled gradient-echo FLASH MR imaging in the detection of patellofemoralar- ticular cartilage abnormalities. Radiology 1996;198:209-12.
22. Disler DG, McCauley TR, Kelman CG, Fuchs MD, Ratner LM, Wirth CR, et al. Fat-suppressed three-dimensional spoiled gradi- ent-echo MR imaging of hyaline cartilage defects in the knee: Comparison with standard MR imaging and arthroscopy. AJR Am J Roentgenol 1996;167:127-32.
23. Eckstein F, Stammberger T, Priebsch J, Englmeier KH, Reiser M.

Effect of gradient and section orientation on quantitative analysis of knee joint cartilage. J Magn Reson Imaging 2000;11:161-7.

24. Alparslan L, Winalski CS, Boutin RD, Minas T. Postoperative magnetic resonance imaging of articular cartilage repair. Semin Musculoskel Radiol 2001;5:345-63.

25. Alparslan L, Minas T, Winalski CS. Magnetic resonance imaging of autologous chondrocyte implantation. Semin Ultrasound CT MR 2001;22:341-51.

26. Kramer J, Recht MP, Imhof H, Stiglbauer R, Engel A. Postcontrast MR arthrography in assessment of cartilage lesions. J Comput Assist Tomogr 1994;18:218-24.

27. Dalla Palma L, Cova M, Pozzi-Mucelli RS. MRI appearance of the articular cartilage in the knee according to age. J Belge Radiol 1997;80:17-20.

28. Link TM, Steinbach LS, Ghosh S, Ries M, Lu Y, Lane N, et al. Osteoarthritis: MR imaging findings in different stages of disease and correlation with clinical findings. Radiology 2003;226:373-81.

29. Gold GE, Hargreaves BA, Stevens KJ, Beaulieu CF. Advanced magnetic resonance imaging of articular cartilage. Orthop Clin North Am 2006;37:331-47, vi.

30. Woertler K, Rummeny EJ, Settles M. A fast high- resolution multislice T1-weighted turbo spin-echo (TSE) sequence with a DRIVen equilibrium (DRIVE) pulse for native arthrographic contrast. AJR Am J Roentgenol 2005;185:1468-70.

31. Mlynarik V, Sulzbacher I, Bittsansky M, Fuiko R, Trattnig S. Investigation of apparent diffusion constant as an indicator of early degenerative disease in articular cartilage. J Magn Reson Imaging 2003;17:440-4.

32. Freeman R. Magnetic resonance in chemistry and medicine. 1st ed. Oxford, UK: Oxford University Press; 2003. p. 280.

33. Mattiello J, Basser PJ, Lebihan D. Analytical expressions for the b- matrix in NMR diffusion imaging and spectroscopy. J Magn Reson Ser A 1994;108:131-41.

34. Miller KL, Hargreaves BA, Gold GE, Pauly JM. Steady-state diffusion-weighted imaging of in vivo knee cartilage. Magn Reson Med 2004;51:394-8.

35. Mamisch TC, Menzel MI, Welsch GH, Bittersohl B, Salomonowitz E, Szomolanyi P, et al. Steady-state diffusion imaging for MR in-vivo evaluation of reparative cartilage after matrix-associated autologous chondrocyte transplantation at 3 tesla)-preliminary results. Eur J Radiol 2008;65:72-9.

36. Kornaat PR, Reeder SB, Koo S, Brittain JH, Yu H, Andriacchi TP, et al. MR imaging of articular cartilage at 1.5T and 3.0T: Comparison of SPGR and SSFP sequences. Osteoarthritis Cartilage 2005;13:338-44.

37. Mlynarik V, Sulzbacher I, Bittsanský M, Fuiko R, Trattnig S. Investigation of apparent diffusion constant as an indicator of early degenerative disease in articular cartilage. J Magn Reson Imaging 2003;17:440-4.

38. Meder R, de Visser SK, Bowden JC, Bostrom T, Pope JM. Diffusion tensor imaging of articular cartilage as a measure of tissue microstructure. Osteoarthritis Cartilage 2006;14:875-81.

39. deVisser SK, Crawford RW, Pope JM. Structural adaptations in compressed articular cartilage measured by diffusion tensor imaging. Osteoarthritis Cartilage 2008;16:83-9.

40. Gold GE, Fuller SE, Hargreaves BA, Stevens KJ, Beaulieu CF. Driven equilibrium magnetic resonance imaging of articular cartilage: Initial clinical experience. J Magn Reson Imaging 2005;21:476-81.

41. Yoshioka H, Alley M, Steines D, Stevens K, Rubesova E, Genovese M, et al. Imaging of the articular cartilage in osteoarthritis of the knee joint: 3D spatial-spectral spoiled gradient-echo vs. fat-suppressed 3D spoiled gradient-echo MR imaging. J Magn Reson Imaging 2003;18:66-71.

42. Disler DG, Peters TL, Muscoreil SJ, Ratner LM, Wagle WA, Cousins JP, et al. Fat-suppressed spoiled GRASS imaging of knee hyaline cartilage: Technique optimization and comparison with conventional MR imaging. AJR Am J Roentgenol 1994;163:887-92.

43. Gold GE, Hargreaves BA, Vasanawala SS, Webb JD, Shimakawa AS, Brittain JH, et al. Articular cartilage of the knee: Evaluation with fluctuating equilibrium MR imaging-initial experience in healthy volunteers. Radiology 2006;238:712-8.

44. Duc SR, Koch P, Schmid MR, Horger W, Hodler J, Pfirrmann CW. Diagnosis of articular cartilage abnormalities of the knee: Prospective clinical evaluation of a 3D water-excitation true FISP se quence. Radiology 2007;243:475-82.

45. Burstein D, Gray ML. Is MRI fulfilling its promise for molecular imaging of cartilage in arthritis? Osteoarthritis Cartilage 2006;14:1087-90.

46. Duc SR, Pfirrmann CW, Koch PP, Zanetti M, Hodler J. Internal knee derangement assessed with 3-minute three-dimensional isovoxel true FISP MR sequence: preliminary study. Radiology 2008;246:526-35.

47. Levitt M. Spin dynamics: Basics of nuclear magnetic resonance. 2nd ed. New York, NY: Wiley; 2008. P. 740.

48. Nissi MJ, Rieppo J, Toyras J, Laasanen MS, Kiviranta I, Nieminen MT, et al. Estimation of mechanical properties of articular cartilage with MRI-dGEMRIC, T2 and T1 imaging in different species with variable stages of matu- ration. Osteoarthritis Cartilage 2007;15:1141-8.

49. Burstein D, Gray ML, Hartman AL, Gipe R, Foy BD. Diffusion of small solutes in cartilage as measured by nuclear magnetic resonance (NMR) spectroscopy and imaging. J Orthop Res 1993;11:465-78.

50. Poon CS, Henkelman RM. Practical T2 quantitation for clinical applications. J Magn Reson Imaging 1992;2:541-53.

51. Li X, Han ET, Ma CB, Link TM, Newitt DC, Majumdar S. In vivo 3T spiral imaging based multi-slice T (1rho) mapping of knee cartilage in osteoarthritis. Magn Reson Med 2005;54:929-36.

52. Wheaton AJ, Borthakur A, Kneeland JB, Regatte RR, Akella SV, Reddy R. In vivo quantification of T1rho using a multislice spin-lock pulse sequence. Magn Reson Med 2004;52:1453-8.

53. Wheaton AJ, Casey FL, Gougoutas AJ, Dodge GR, Borthakur A, Lonner JH, et al. Correlation of T1rho with fixed charge density in cartilage. J Magn Reson Imaging 2004;20:519-25.

54. Regatte RR, Akella SV, Lonner JH, Kneeland JB, Reddy R. T1rho relaxation mapping in human osteoarthritis (OA) cartilage: Comparison of T1rho with T2. J Magn Reson Imaging 2006;23:547-53.

55. Bashir A, Gray ML, Boutin RD, Burstein D. Glycosaminoglycan in articular cartilage: In vivo assessment with delayed Gd (DTPA)(2) enhanced MR imaging. Radiology 1997;205:551-8.

56. Mlynarik V, Sulzbacher I, Bittsansky M, Fuiko R, Trattnig S. Investigation of apparent diffusion constant as an indicator of early degenerative disease in articular cartilage. J Magn Reson Imaging 2003;17:440-4.

57. Hancu I, Boada FE, Shen GX. Three-dimensional triple-quantum-filtered (23) Na imaging of in vivo human brain. Magn Reson Med 1999;42:1146-54.

58. Takahashi M, Uematsu H, Hatabu H. MR imaging at high magnetic fields. Eur J Radiol 2003;46:45-52.

59. Katta J, Jin Z, Ingham E, Fisher J. Biotribology of articular cartilage: A review of the recent advances. Med Eng Phys 2008;30:1349-63.

60. Gold GE, Hargraeves BA, Reeder SB, Vasanawala SS, Beaulieu CF, Controversies in protocol selection in the imaging of articular cartilage. Semin Musculoskelet Radiol 2005;9:161-72.